Introducing quantum mechanics through its historical roots: The hydrogen Rydberg atom viewed through the lens of the old quantum theory

M. G. Littman,[a] E. Gordis,[b] P. Zhelnin,[c] and J. Arnold[d]
Mechanical and Aerospace Engineering, Princeton University, Princeton, New Jersey 08544

(Received 6 April 2022; accepted 25 February 2023)

Solutions of Schrödinger's equation for Rydberg states of hydrogen are shown to display patterns that can be understood semi-classically within the framework of Bohr-Sommerfeld planetary orbits and de Broglie's concept of matter waves. Using $n = 10$ and $n = 100$ quantum levels we show how de Broglie-wave-analyzed Kepler orbits can be matched to excited-state wavefunctions and charge distributions. Making the connection between the old and new quantum theories can help beginning students develop an intuition about quantum mechanics and allow them to develop an appreciation of how Schrödinger's wave mechanics was stimulated by the theories of his predecessors.
https://doi.org/10.1119/5.0094860

I. CIRCULAR ORBITS AND "CIRCULAR STATES"

Niels Bohr's 1913 paper described an analytical method that built upon Ernest Rutherford's concept of an atom as a positively charged nucleus surrounded by a system of negatively charged electrons.[1] An early success of Bohr's atomic theory was its ability to derive and explain the empirical formula of Johannes Rydberg for the frequencies of spectral lines of atomic hydrogen.[2] Bohr analyzed the hydrogen atom as a single electron orbiting an infinitely massive positive nucleus (that is, a single proton). He simplified the problem by assuming further that the electron orbit was circular. Bohr used non-relativistic classical mechanics as the foundation for his analysis, but he also drew upon the work of Max Planck to understand radiation associated with an orbiting electron. Planck earlier had proposed the concept of the energy-quanta to explain blackbody radiation.[3] In Bohr's model, rather than an orbiting electron radiating energy continuously, he suggested that radiation from excited hydrogen occurred in distinctly separated emissions (described today as jumps) between stationary states. Stationary states of hydrogen were those that satisfied an integer condition connected with Planck's idea of quantized action.

Bohr designated the integer factor in his analysis with τ—we will instead use n, which is known commonly as the principal quantum number. Bohr showed that the energy of the stationary states is proportional to $-1/n^2$, and the angular momentum of the stationary states is $nh/2\pi$, where h is Planck's constant. Bohr identified a most tightly bound state (the ground state) corresponding to the smallest possible positive integer, $n = 1$. The radius of the circular orbits according to Bohr's model is $n^2 a_0$, where a_0 is the Bohr radius. The model also shows that the electron velocity in an orbit is $v/c = (1/n)(2\pi e^2/(4\pi\varepsilon_0 hc))$. (Here, ε_0 is the permittivity of free space.[4]) The numerical factor in the velocity relationship is Sommerfeld's fine structure constant, $\alpha = 2\pi e^2/(4\pi\varepsilon_0 hc) \approx 1/137$. The velocity scales as $1/n$. The energy of stationary states of the electron according to the Bohr model is $-(hcR_\infty)/n^2$, where R_∞ is the Rydberg constant and c is the speed of light. Bohr's derived formulas for both a_0 and R_∞ were given in terms of fundamental constants: the electron mass, m_0; the electron charge, e; and Planck's constant, h. Bohr's value for R_∞ based on fundamental constants is very close to Rydberg's experimentally determined value.

The notion of a moving electron as a wave is often invoked in modern explanations of Bohr's quantum theory, but the concept did not emerge until about 10 years after Bohr's landmark paper. Bohr only introduced a stability condition. Louis de Broglie, drawing on the works of Maupertuis (principle of least action) and Fermat (principle of least time), reasoned that particles following a trajectory have a wave nature. In a paper published in 1925, de Broglie noted the connection between the concept of a particle wave and Bohr's stability condition:[5] "Propagation is, therefore, analogue to a liquid wave in a channel closed on itself but of variable depth. It is physically obvious, that to have a stable regime, the length of the channel must be resonant with the wave; …The resonance condition is $L = n\lambda$ if the wavelength is constant …" [L is de Broglie's value for the length of the channel and n is an integer.] Then he continued in a later paragraph, "In the particular case of closed circular Bohr orbits in an atom, one gets: $m_0 \oint v dL = 2\pi R\, m_0 v = nh$, where $v = R\omega$, when ω is angular velocity, $m_0 \omega R^2 = nh/2\pi$. This is exactly Bohr's fundamental formula." Since the circumference of the Bohr circle is $2\pi R$, the wavelength extracted from Bohr's formula is $\lambda = h/m_0 v$, that is, de Broglie's well known relationship. We see that the circular Bohr orbit contains n electron wavelengths, and the electron phase is a multiple of 2π at n points equally spaced along the orbit.

Now we consider the Schrödinger wavefunction, which in a spherical basis (r, θ, φ) is characterized by the quantum numbers, n, ℓ, and m. We will focus on the "circular state"[6] of quantum level n, which has maximal values of both ℓ and m, namely, $\ell = n - 1$ and $m = \pm\ell$. Since we compare orbits to a slice of the wavefunction, it is helpful first to consider the bigger picture of what the electron charge distribution looks like for the $n = 10$ "circular state." This is given in Fig. 1, which shows in 3D that the distribution appears as a torus centered on the origin. The charge density peaks at a radius somewhere between the inner and outer radii of the torus.

The sum of the squares of the real and the imaginary parts of the wavefunction is used to compute the probability density in Fig. 1. Figure 2 is a 2D contour plot of the real part of the wavefunction in the $x - y$ plane. Red contours are for

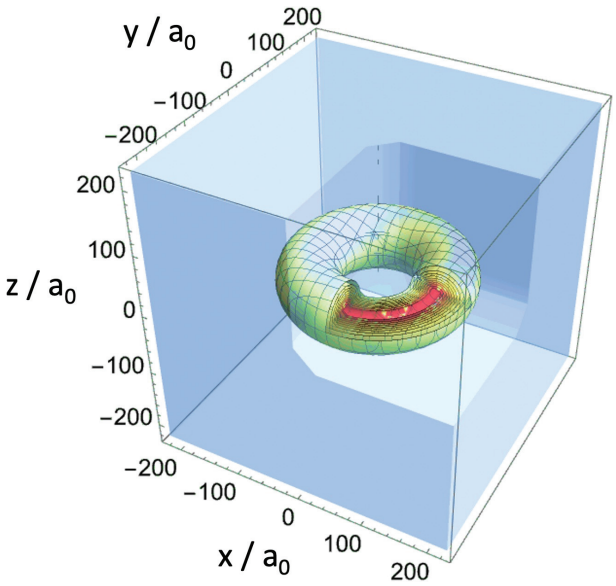

Fig. 1. A 3D contour plot of the electron charge probability density for the $n = 10$ "circular state" of hydrogen. Here, $\ell = 9$, and $m = \pm 9$. The charge probability density is given by the wavefunction multiplied by its complex conjugate. One upper quadrant of the 3D contour plot has been removed to show that the charge density is largest near the middle of the torus. a_0 is the Bohr radius.

positive real values. Blue dashed contours are for negative real values. Black lines indicate where the real part of the wavefunction is zero.

The imaginary part of the wavefunction in the $x - y$ plane has the same pattern as the real part shown in Fig. 2 but is rotated about the z-axis by $+10^\circ$ (CCW) for the $m = +9$ state and by -10° (CW) for the $m = -9$ state. Because the $n = 10$ "circular state" has 9-fold symmetry, a spatial rotation of 40° (that is, $360^\circ/9$) in either the CCW or CW direction about z will leave the complex wavefunction unchanged. The $\pm 10^\circ$ relative rotation between real and imaginary parts means that the azimuthal pattern of the real and imaginary parts oscillates and is in quadrature (that is, one quarter of the way to the symmetry rotation). This is fundamental.[7] It allows the sum of the squares of real and imaginary parts to be constant as a function of the azimuthal angle ϕ. We are interested in using orbits to understand spatial patterns in wavefunctions. Since the patterns of real and imaginary parts differ only by a rotation, we restrict our comparison, without loss of generality, to the real part of the wavefunction. All subsequent mention of the wavefunction, therefore, will be the real part only.

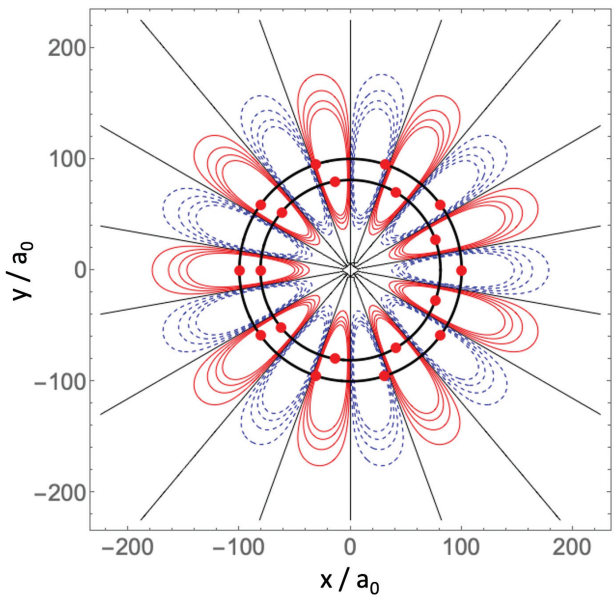

Fig. 2. Contour plot of the real part $n = 10$, $\ell = 9$, $m = \pm 9$ "circular state" wavefunction evaluated in the $x - y$ plane. The imaginary part of the wavefunction has an identical pattern but is rotated about the z-axis by $\pm 10^\circ$. The relative rotation means that the maxima of the imaginary part exactly coincide with nodes of the real part and vice versa. The red-colored contour lines correspond to the positive real value of the wavefunction, and blue-colored-dashed lines correspond to the negative real values. Black lines indicate where the real part of the wavefunction is zero. Shown also are Bohr's orbits for $n = 9$ and $n = 10$. The red dots are placed where the electron phase is a multiple of 2π. Each arc segment of the Bohr orbit is the electron wavelength in that orbit. There are nine electron wavelengths in the $n = 9$ orbit and ten electron wavelengths in the $n = 10$ orbit. a_0 is the Bohr radius.

We now compare Schrödinger's wavefunction for $n = 10$ "circular states" with Bohr's circular orbit for $n = 9$ and $n = 10$. Why consider $n = 9$? We include the $n = 9$ orbit because Schrödinger and Bohr analyses differ in their values for angular momentum. Schrödinger's value of angular momentum for "circular states" of quantum level n is $(n - 1)h/2\pi$, whereas the circular orbits of Bohr for quantum level n have angular momentum $nh/2\pi$, that is, $h/2\pi$ larger. The Bohr method overestimates angular momentum of each quantum level—this well-known flaw of Bohr's theory[8] was corrected by Schrödinger in 1926.[9] This error leads Bohr to assume that the angular momentum of the $n = 1$ ground state is $h/2\pi$, whereas Schrödinger's ground state has angular momentum zero. So, we will start by considering both $n = 9$ and $n = 10$ Bohr orbits in comparison with the $n = 10$ "circular state." Plotted in Fig. 2 are contours of the Schrödinger wavefunction in the $x - y$ plane as compared with these two Bohr orbits.

We see that while the $n = 10$ Bohr orbit does a good job at matching the anti-node peaks of the real part of the wavefunction, the red dots in that orbit miss the wavefunction phase (that is, the oscillations)—whereas the red dots of the $n = 9$ Bohr orbit do a good job at matching the phase – they do this because the angular momentum for the $n = 9$ Bohr case matches the angular momentum (and the symmetry) of the $n = 10$ circular Schrödinger case. Our approach then for comparing Schrödinger $n = 10$ results to the Bohr model is to use the $n = 9$ orbit but scaling it up in physical dimension by the factor, 100/81. Now both the size of the orbit and the phase will line up as shown in Fig. 4(a). For comparisons with states of higher values of n, for example, $n = 100$, as considered in Sec. III of this paper, the scaling is not necessary because the scale factor, $(n^2)/(n - 1)^2$, approaches 1 when n is very large, but we still will use a quantum number for Bohr orbits that is one less than that of the Schrödinger state.

II. ELLIPTICAL ORBITS AND SPHERICAL STATES

In 1916, Sommerfeld expanded Bohr's approach by including the possibility of elliptical orbits.[10–12] This possibility corrected a shortcoming of Bohr's model by providing an analysis that improved comparison with experimentally observed level splitting due to external electric and magnetic fields. To allow elliptical orbits, Sommerfeld postulated a new quantum stability condition involving multiple quantum numbers, that is, a quantum condition for each degree of freedom for an orbit of an electron. He assumed that the orbit was confined to a plane, and therefore, there were two quantum conditions and two quantum numbers.

Here, we compare the Bohr–Sommerfeld planar elliptical orbits with the solutions of atomic wavefunctions. To begin, we restrict our attention to the $x-y$ plane and consider only Bohr–Sommerfeld orbits in that plane. The classical angular momentum is perpendicular to the orbital plane. Thus, for these orbits, the angular momentum points along the z axis. The Sommerfeld method, like that of Bohr, overestimates the total angular momentum by $h/2\pi$. In a state with principal quantum number n, the maximal values for the quantum numbers ℓ and m are $n-1$. So, as in Sec. I, when we compare the Bohr–Sommerfeld model to the Schrödinger equation solutions, we compare cases of the same angular momentum with the same projection of angular momentum along the z axis. Therefore, we match Bohr–Sommerfeld orbits having quantum number, $n-1$ (which have ℓ values that range from 1 to $n-1$) to Schrödinger wavefunctions for states having quantum number, n (with ℓ values that also range from 1 to $n-1$—the $\ell=0$ case is not considered). We also restrict the comparison to those m states that have the maximum angular momentum projection along z—that is, $m=\pm\ell$, for each case.

Sommerfeld noted that Bohr's circular orbits have only one degree of freedom and that made it relatively easy to apply Planck's quantized action condition. The elliptical case for motion in a plane involves two degrees of freedom, and, therefore, he postulated that the quantized action conditions for stability should also have two conditions: $\oint p_\theta\, d\theta = n_\theta h$ and $\oint p_r\, dr = n_r h$, where $n_\theta + n_r = n$. Here, $p_\theta = m_0 r^2 d\theta/dt$ is the moment of momentum, and $p_r = m_0 dr/dt$ is the radial component of momentum, which is m_0 times the radial velocity. Following this approach, he concluded that there are n orbits that satisfy the stability condition for the quantum level n: the circular orbit and $n-1$ additional elliptical orbits. The possible solutions have angular momenta ranging from $nh/2\pi$ down to $h/2\pi$. These correspond to n_θ ranging from n down to 1. The case $n_\theta = n$ is Bohr's circular orbit. Sommerfeld eliminated the case of $n_\theta = 0$ arbitrarily, arguing that this case would have the electron collide with the nucleus. Sommerfeld computed the $n=4$ case as an example. He noted that the circle and all the ellipses share a common semi-major axis, $n^2 a_0$. Figure 3(a) is an image taken directly from Sommerfeld's original paper.[10]

As with our treatment of circular orbits and "circular states," we compare the size and phase of elliptical orbits with Schrödinger's spherical states. To find the phase, we need to determine the electron velocity. For elliptical orbits, the velocity is not constant in time, so we need to solve the classical Kepler problem.[13] Knowing how the velocity varies along the orbit will allow us then to determine the locations along the elliptical path where the phase is a multiple of 2π. MATHEMATICA is used to solve for the Kepler orbits according to the parametric equations

$$x(\theta) = a(\cos\theta - \varepsilon), \tag{1}$$

$$y(\theta) = b\sin\theta, \tag{2}$$

$$M = \omega t = \theta - \varepsilon\sin\theta. \tag{3}$$

Here, ε is the eccentricity, a is the semi-major axis of the ellipse, b is the semi-minor axis of the ellipse, ω is the orbital frequency in radians/seconds, and M is the mean anomaly. The equation for M is Kepler's equation. Sommerfeld's model provides expressions for a, b, ε, and ω in terms of n and ℓ: $a = n^2 a_0$; $b = n\ell a_0$; $\varepsilon = \sqrt{(1-(b^2/a^2)}$; and $\omega = (m_0 e^4)/((4\pi\varepsilon_0)^2 (h/2\pi)^3 n^3)$. To solve for $x(t)$ and $y(t)$, we invert Kepler's equation to solve for $\theta(t)$. This cannot be done analytically—so we invert it numerically using the "InverseFunction" function in MATHEMATICA. Once we have $\theta(t)$, we make a table of $\theta(t)$, $x(t)$, and $y(t)$. This table is based on a time step of typically 10^{-4}–10^{-6} of the orbital period. The table entries let us solve for the electron velocity along the elliptical path.

To figure out the points along the path where the phase advances by a multiple of 2π, we rely on the action phase-integral, $(\oint pdq)/h$. We assume a single degree of freedom for the electron as it moves along the ellipse. To get p at time step $t+\Delta t$, we use the chain rule. We differentiate Eqs. (1) and (2) with respect to θ and determine $d\theta/dt$ by differentiating Eq. (3). Then $p = m_0(d\theta/dt)\sqrt{([dx/d\theta]^2 + [dy/d\theta]^2)}$, and $dq = d\theta\sqrt{([dx/d\theta]^2 + [dy/d\theta]^2)}$. We determine $d\theta$ by taking the differences in the table for $\theta(t)$ at times $t+\Delta t$ and t. We start at the perihelion (the point of closest separation between the electron and the nucleus) and define the phase at that point to be equal to zero. The phase tabulation begins at $t=0$. The electron moves along the elliptical path, and for each new time step, we record the accumulated phase in an additional column in the table. We plot the orbit using the $x(t)$ and $y(t)$ values in the table and place a red dot at those points where the accumulated phase reaches a multiple of 2π.

This was done for the $n=4$ case as shown in Fig. 3(b). As expected, when the electron is moving quickly near the perihelion, the electron wavelength is smaller than it is when near the aphelion (the most distant separation between

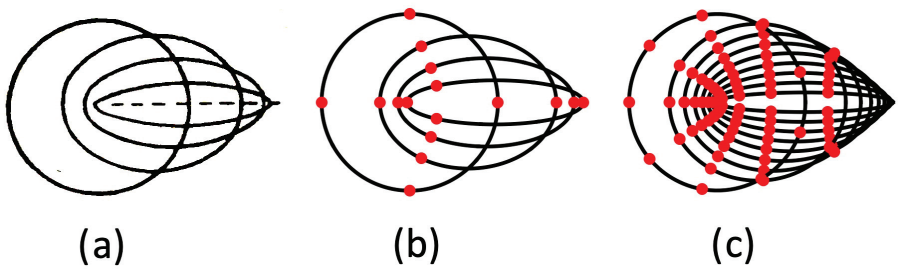

Fig. 3. (a) Sommerfeld's orbits for hydrogen in the $n=4$ level. Angular momentum of the orbits is $4h/2\pi$, $3h/2\pi$, $2h/2\pi$, and $h/2\pi$. This image is from Sommerfeld's original 1916 paper (Ref. 10); (b) Sommerfeld's allowed orbits for hydrogen in the $n=4$ level. Red dots indicate locations where the electron phase is a multiple of 2π. Each arc segment is one electron wavelength. There are four electron wavelengths in the circular orbit and in each of the elliptical orbits; (c) Sommerfeld's allowed orbits for hydrogen in the $n=9$ level. Angular momentum of the orbits is $9h/2\pi$, $8h/2\pi$, …, $2h/2\pi$, $h/2\pi$. Red dots indicate locations where the electron phase is a multiple of 2π. There are nine electron wavelengths in the circle and in each of the ellipses.

electron and the nucleus). For $n=4$, there are four electron wavelengths in the circular orbit and in each of the ellipses.

In Fig. 3(c), we have done this also for the $n=9$ case. Here, there are nine electron wavelengths in the circular orbit and in each of the eight additional ellipses. This family of orbits will be used to compare with the $n=10$ Schrödinger wavefunctions.

Now we overlay the scaled $n=9$ Bohr–Sommerfeld orbits on the $n=10$ Schrödinger wavefunctions. We do this for each of the possible ℓ values (leaving out $\ell=0$—so $\ell=9,8,\ldots,2,1$). The comparisons are for equal values of ℓ and only for the sub-levels that have a maximum projection of angular momentum on the z axis. Thus, if we are making comparisons for the $\ell=9$ state, we choose $m=\pm 9$. If we are comparing the $\ell=8$ state, we choose $m=\pm 8$ for comparison, and so on. In Fig. 4, n= 9 Bohr–Sommerfeld orbits are overlayed on $n=10$ Schrödinger wavefunctions for four cases.

Figure 4(a) is the circular state, $n=10,\ell=9,m=\pm 9$, compared to the $n=9$ Bohr and Sommerfeld model solution. The state $n=10,\ell=8,m=\pm 8$, shown in Fig. 4(b), displays several interesting features. It has 8-fold symmetry, one less than the $n=10,\ell=9,m=\pm 9$ state. Along the radial direction, a second ring of anti-nodes appears. Recall Sommerfeld's suggestion of two quantum numbers, n_θ and n_r—so the reduction of the circumferential symmetry by 1 and the increase in the radial rings by 1 is consistent with Sommerfeld's idea that $n_\theta+n_r=n$. As we will see for lower ℓ states, as the circumferential symmetry drops by 1, the ring of radial anti-nodes will increase by 1. Next, we see that the perihelion of the elliptical orbit aligns with the location of the inner ring. This trend will continue with lower ℓ states. Each time a new inner ring is added by decreasing ℓ, the location of the inner-most ring of anti-nodes will match the location of the perihelion of the elliptical orbit. We see also that there is rough correspondence with the location of the positive circumferential anti-nodes with the red dots along the ellipse.

Note that the overall size of the Schrödinger $n=10$, $\ell=8,m=\pm 8$ wavefunction appears larger than the $n=10,\ell=9,m=\pm 9$ wavefunction. This can be seen as the result of sweeping the ellipse about the nucleus—recall that the semi-major axis of all of the ellipses and the circle is n^2a_0. According to Bethe and Salpeter,[14] the average value of the radius for a Schrödinger state of angular momentum ℓ is $(1/2)(3n^2-\ell(\ell+1))a_0$. That is, the smaller ℓ, the larger the average size of the state—only when ℓ is $n-1$ does the size of the state approach the classical value of n^2a_0. So according to this relationship, the average radius of Schrödinger's $n=10,\ell=9$ state is $105a_0$ (as compared to $100a_0$), and the radius of the $n=10,\ell=8$ state is $114a_0$ (a larger value than $105a_0$). The expected average radius of the $n=10,\ell=1$ state should be $149a_0$ (that is, 50% larger than $100a_0$).

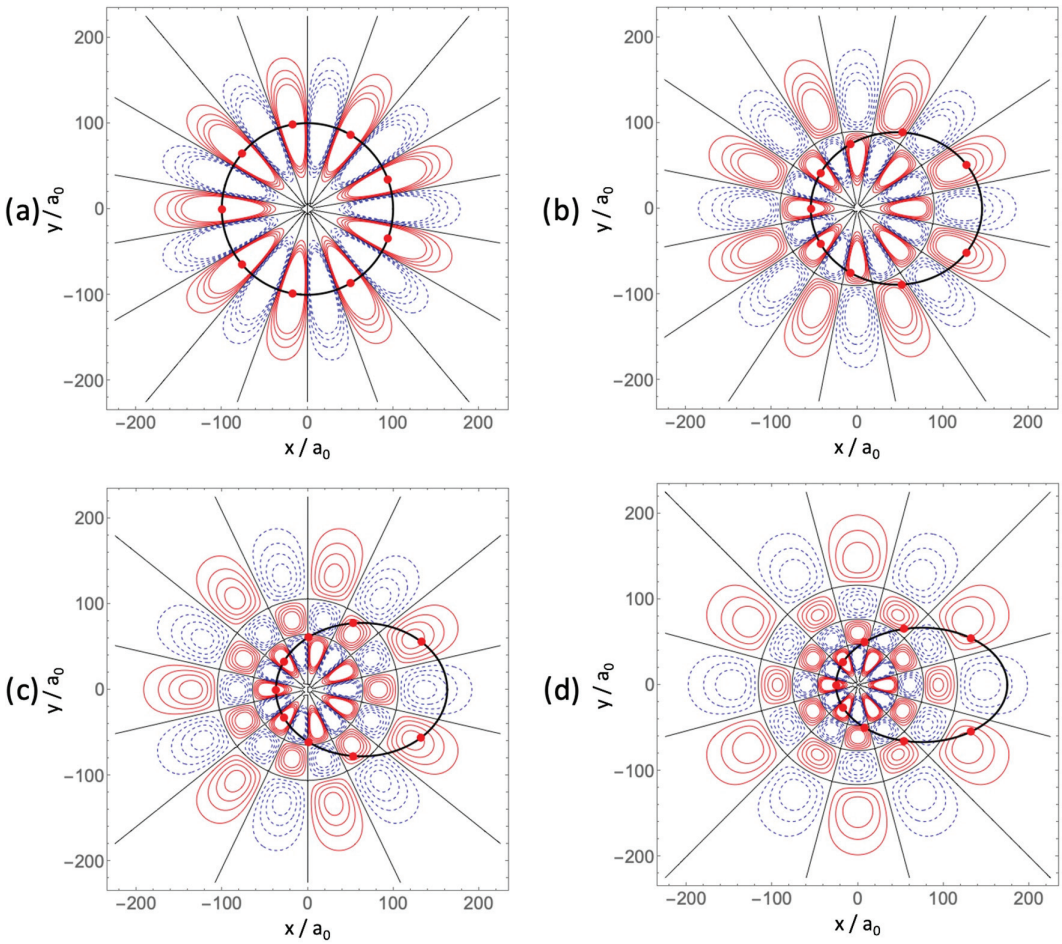

Fig. 4. Sommerfeld orbits for $n=9$ (scaled by 100/81) overlayed on contour plots of the Schrödinger wavefunction for $n=10$; (a) $\ell=9$, $m=\pm 9$; (b) $\ell=8$, $m=\pm 8$; (c) $\ell=7$, $m=\pm 7$; (d) $\ell=6$, $m=\pm 6$. Note that as the ℓ value decreases, the circumferential symmetry decreases, and the number in radial rings increases. Note also that the perihelions of the orbits align with the innermost rings of the Schrödinger wavefunctions. a_0 is the Bohr radius.

The next two wavefunctions in the $n = 10$ sequence are $\ell = 7, m = \pm 7$, and $\ell = 6, m = \pm 6$, shown in Figs. 4(c) and 4(d). These states also match up with the de Broglie-wave-analyzed orbits. The lower ℓ states ($\ell = 4, 3, 2$, and 1) continue to follow these trends—as the ℓ value decreases, the circumferential symmetry decreases, and the number of radial rings increases. All this is consistent with Sommerfeld's hypothesis that $n_\theta + n_r = n$.

One of the reviewers of this paper asked if the correlation of the de Broglie phase between the Bohr and Bohr–Sommerfeld models and the actual Schrödinger wavefunctions is significant or merely coincidence? This is a good question worthy of discussion.

We know that classical elliptical orbits have been used with much success to understand quantum mechanical behavior of hydrogen and hydrogen-like atoms. For example, Horbatsch, Hessels, and Horbatsch in their paper entitled, "Classical calculation of the lifetimes and branching ratios for radiative decays of hydrogenic atoms,"[15] found that they could accurately estimate quantum mechanical radiative decay in hydrogen using semi-classical methods for all states having principal quantum numbers n and $\ell \geq 1$. They assumed that each n, ℓ state had a single well-defined eccentricity that depended on the energy of the state and its angular momentum. Their agreement for lifetimes was excellent ($<$100 parts per million error for $\ell \geq 30, < 0.1\%$ for $\ell \geq 9, < 1\%$ for $\ell \geq 3$), and their agreement for branching ratios was quite reasonable. Their calculation was based on Larmor radiation of a circulating electron in orbit around the nucleus. This same type of calculation is posed in a question at the end of Chapter 14 of Jackson's *Classical Electrodynamics* textbook.[16] In addition to the study of lifetimes and branching ratios, there are other successful studies using classical orbits to analyze quantum phenomenon in hydrogen, and recent studies give us confidence that looking for elliptical orbits where the eccentricity is well defined is sensible and not likely due to coincidence.

However, perhaps the best test is whether the method works with other sublevels. So, in response to a reviewer's query, we examined the wavefunctions for another group of states, namely, $m = 0$ states having $\ell = 9, 8, \ldots, 2, 1$. We found that all of the $m = 0$ wavefunctions follow the same patterns as the case discussed earlier, but now the patterns lie in any plane that contains the z axis. In the $m = 0$ case, the classical Bohr–Sommerfeld orbit used for comparison with the quantum result will lie in the same z-axis-containing plane. Since the angular momentum vector is perpendicular to the orbital plane, the projection of the angular momentum along z is also zero. Shown in Fig. 5 are two of these patterns for the case of $\ell = 5$. The one on the left is the wavefunction pattern in the $x - y$ plane for the $m = \pm 5$ sublevels, and the one on the right is the wavefunction pattern in the $x - z$ plane for the $m = 0$ sublevel. The two are strikingly similar. With these additional states, we find now that 27 of the 100 sublevels of $n = 10$ quantum level have patterns of nodes and antinodes that can be explained using these semi-classical ideas. Observe that the charge distributions for the $m = 0$ case and the $m = \pm 5$ cases are very different from one another—the charge distribution of the $m = 0$ case is a collection of spherical rings, whereas the charge distributions of the $m = \pm 5$ cases are planar rings. These are shown in Fig. 6. It is evident that the semi-classical analysis can help one understand nodal patterns in charge distributions as well as in wavefunctions.

III. ELLIPTICAL ORBITS AND SPHERICAL STATES—CHARGE DISTRIBUTIONS COMPARED RADIALLY

Using the method of separation of variables, the Schrödinger wavefunction for hydrogen can be factored into two parts, $R_{n\ell}(r)$ and $Y_{\ell m}(\theta, \varphi)$. Here, $R_{n\ell}(r)$ is the solution to the hydrogen radial equation. $Y_{\ell m}(\theta, \varphi)$ are the spherical harmonics. Because of this factorization, we can determine the charge probability density distribution as a function of r. The Schrödinger radial distribution is given by $r^2[R_{n\ell}(r)]^2$. Our objective in this section is to compare this radial distribution to the radial distribution expected for de Broglie-wave-analyzed Bohr–Sommerfeld orbits. We will be able to do this because Sommerfeld's stability conditions are in two

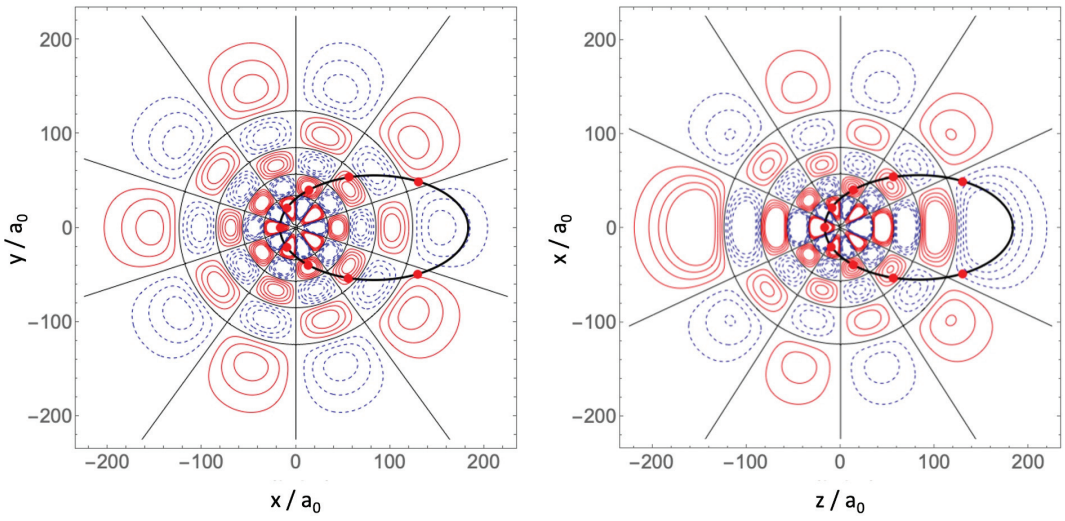

Fig. 5. Schrödinger wavefunctions for $n = 10$ states with $\ell = 5$. Left is an $x - y$ slice for the $m = \pm 5$ sublevels, and right is an $x - z$ slice for the $m = 0$ sublevel. To facilitate comparison with the image on the left, the $x - z$ slice is rotated 90° with the z axis horizontal. For the $m = 0$ case, a slice in any plane containing the z axis will appear the same. The nodal patterns of these different cases are similar. Both wavefunctions roughly match the size and phases of the overlayed $n = 9, \ell = 5$ Bohr-Sommerfeld orbit.

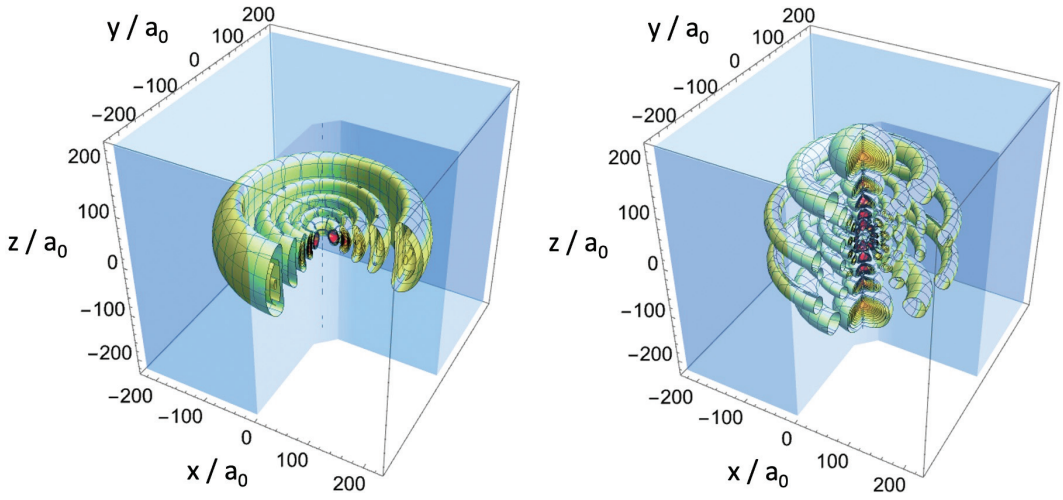

Fig. 6. 3D contour plots of the charge probability density distribution for $n = 10$, $\ell = 5$ states. Left is the distribution corresponding to $m = \pm 5$ sublevels, and right is the distribution corresponding to the $m = 0$ sublevel.

parts: one that is radial and another that is azimuthal. This quantum-classical comparison has two aspects. One involves matching the amplitude envelope of the quantum probability density to a classical analysis of the radial probability density for Kepler orbits. The other involves matching the phase.

To match the amplitude envelope, we note that the radial probability density for a classical electron in orbit is proportional to $1/[dr/dt]$, which for Keplerian orbits is known to be $r/(\pi a\sqrt{(\varepsilon^2 a^2 - (r-a)^2)})$, where ε is the eccentricity and a is the size of the semi-major axis of the ellipse.[17,18] Comparisons between the amplitude envelope and the classical radial probability distribution have been noted by authors in previous works.[17,19,20]

To get the de Broglie phase, we apply Sommerfeld's radial stability condition: $\oint (p_r/h)dr = n_r$. Here, p_r is $m_0 dr/dt$. We tabulate $r(t)$ in a Bohr–Sommerfeld orbit in a manner similar to that in Sec. II, using $r(t) = \sqrt{[x(t)]^2 + [y(t)]^2}$, where $x(\theta(t))$ and $y(\theta(t))$ are given in Eqs. (1) and (2). We get dr/dt by applying the chain rule, $dr/dt = (dr/d\theta)(d\theta/dt)$, and $dr = [(dr/dt)(dt)]$. $d\theta/dt$ is determined by differentiating Eq. (3). Previously with the phase integral along the ellipse, we noted every time the phase advanced to a multiple of 2π, but in this case, we will note the values of r where the phase advances to a multiple of π because we are plotting the probability density rather than the wavefunction. Note that the method here considers only the radial path, r, using the differential radial phase of $(p_r/h)dr$. In contrast, in Sec. II, the method for determining the phase was based a one-dimensional elliptical path, q, using the differential electron phase, $(p/h)dq$.

In Fig. 7, the radial charge distribution for the $n = 100$, $\ell = 80$ Schrödinger state is compared to the classical probability distribution for the n $= 99, \ell = 80$ Bohr–Sommerfeld orbit. The classical distribution is the solid black line. This figure also has red dots placed at the radii, where the phase advances by multiples of π. The semi-classical result helps one to understand aspects of the quantum result. One sees that the average amplitude of the oscillatory solution matches the classical value. One also sees that the anti-nodes of the oscillatory solution are in reasonable correspondence with the red dots. We are using the $n = 99$ Bohr–Sommerfeld orbit for comparison here for the same reasons that we did in Secs. I and II. In this case, the $n = 99$ Bohr–Sommerfeld orbital size is very close to the $n = 100$ orbital size, so there was no need to scale the results as we did previously.

IV. ELLIPTICAL ORBITS AND PARABOLIC STATES

Sommerfeld used parabolic coordinates for his comparisons to the Stark effect. He used the Hamilton–Jacobi method of separation of variables to develop three quantum stability conditions according to the parabolic coordinate variables ξ, η, and ϕ. These stability conditions gave rise to quantum numbers, n_1, n_2, and m. Schrödinger's equation can be analyzed using parabolic coordinates and also using the method of separation of variables. As pointed out by Bethe and Salpeter,[14] the form of the perturbation potential for the electric field along the z axis preserves the method of separation of variables since the variable z is a linear combination of ξ and η, namely, $z = 0.5(\xi - \eta)$. The other variables are $x = \sqrt{\xi\eta}\cos(\phi)$; $y = \sqrt{\xi\eta}\sin(\phi)$; and $\phi = \arctan(y/x)$.

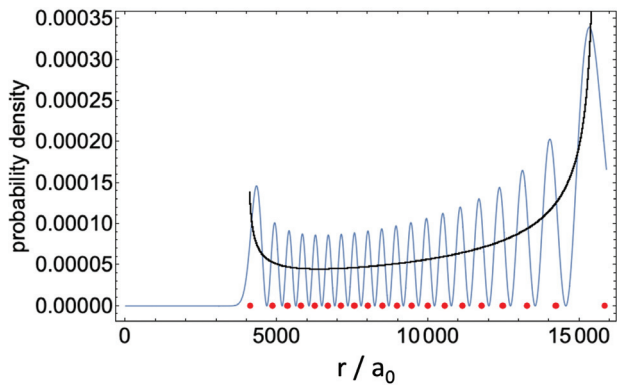

Fig. 7. The blue line is the Schrödinger radial charge distribution for quantum level $n = 100, \ell = 80$. The black line is the classical probability distribution as a function of radius for an electron following an $n = 99, \ell = 80$ Bohr-Sommerfeld orbit. The horizontal axis is in atomic units, a_0. The red dots mark the radii according to the de Broglie phase wave idea, where the phase reaches a multiple of π. The calculation begins at the perihelion with phase equal to zero. The red dots roughly correlate with the anti-nodes of the radial charge density. a_0 is the Bohr radius.

Parabolic states are used often to analyze the Stark effect in atomic hydrogen. For a state to have a linear shift in the electric field, it means that in the absence of a field, there would be an electric dipole moment. That is true for parabolic states but not for spherical states, which are symmetric or antisymmetric with respect to inversion. The energy shift of a state with an electric dipole moment is the product of the electric dipole moment and the external field. If the state has an electric dipole moment in the absence of a field, then application of an external field leads to a shift that is linear in the field—that is what happens in excited atomic hydrogen.

Figure 8 is a contour plot of the charge distribution of a parabolic state for the quantum level, $n = 10$ in the $x - z$ plane. This state has the largest electric dipole moment of the 100 sub-levels of $n = 10$ and the largest linear shift in an external electric field–it also has $m = 0$. A Bohr–Sommerfeld ellipse in the $x - z$ plane has its angular momentum vector along the y axis and, therefore, would also have $m = 0$. We know from Schrödinger's analysis that parabolic states do not have a well-defined angular momentum. Instead, they are made up of a superposition of multiple angular momentum states.[19] The fractional component is determined by projecting the parabolic state onto spherical states of various values of ℓ. One can develop insight about the Schrödinger result if we compare a collection of Bohr–Sommerfeld elliptical orbits to an $x - z$ slice of the Schrödinger charge distribution—we could have also used a $y - z$ slice, or any slice that contains the z axis—this state has rotational symmetry about z. In Fig. 8, four Bohr–Sommerfeld orbits having $\ell = 1, 2, 3,$ and 4 are overlayed on the quantum charge distribution. For these four Bohr–Sommerfeld orbits, the angular momentum vector points along y. The contours shown are for a slice in the $x - z$ plane. The red dots appear at multiples of π in phase along the orbits. You will note that the anti-nodes of the parabolic state roughly line up with the red dots. We see that the size and de Broglie phase of the classical elliptical orbit help one to understand both the oscillations and the amplitude of the quantum charge density.

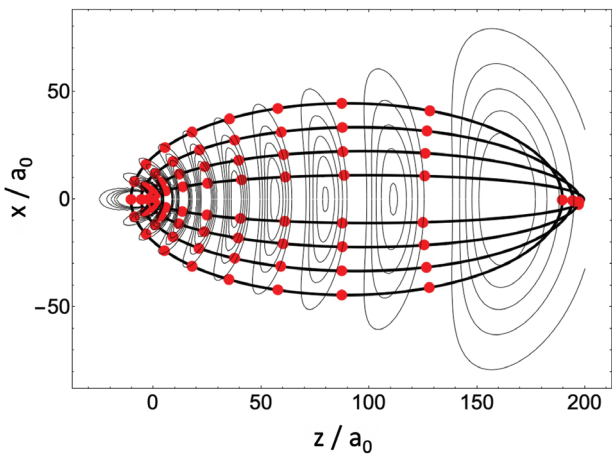

Fig. 8. $x - z$ slice of the charge distribution for an $n = 10$ parabolic state $(n_1 = 9, n_2 = 0, m = 0)$ overlayed with a scaled (100/81) group of $n = 9$ Bohr–Sommerfeld orbits having $\ell = 1, 2, 3,$ and 4. The angular momentum of all these orbits lies along the y axis. This state has the largest electric dipole moment of all of the $n = 10$ sub-levels; Here, the cycle-averaged center of the electric charge is far to the right of the nucleus. The dots indicate the locations, where the de Broglie phase advances by π. Note that dots roughly align with the anti-nodes of the charge distribution. This state has rotational symmetry about the z axis, so a slice in any plane that includes the z axis will give the same charge distribution.

V. CONCLUSIONS

Wavefunctions and charge densities for atomic hydrogen display patterns that are understandable in terms of the planetary models of the old quantum theories. The seemingly complex myriad of nodes and anti-nodes of hydrogen are recognizable in comparison with de Broglie-wave-analyzed Bohr–Sommerfeld orbits. One need not dismiss the old quantum theories so quickly when teaching or studying quantum mechanics. Appreciation of physical ideas like the de Broglie phase wave can help students look for features in quantum solutions that trigger their imagination. How might a classical orbiting electron behave? If the wavefunction or the charge distribution is rapidly changing in space, then the classical interpretation is that the electron is moving quickly. Schrödinger's 1926 paper in the *Physical Review*[9] reminds us of how important classical mechanics and de Broglie's ideas were in his developing wave mechanics. He started off his paper as follows: "The theory which is reported in the following pages is based on the very interesting and fundamental researches of L. de Broglie on what he called 'phase wave' ('ondes de phase') and thought to be associated with the motion of material points, especially with the motion of an electron or proton. The point of view taken here, which was first published in a series of German papers, is rather that material points consist of, or are nothing but, wave-systems." Schrödinger was inspired by classical motion and the phase waves of de Broglie. So, too, can these ideas help the beginning student see the connections between quantum solutions and classical ideas and help the student to develop an understanding of why quantum wavefunctions and charge distributions look the way they do.

ACKNOWLEDGMENTS

The authors thank Marko Horbatsch of York University for helpful discussions. The authors are also grateful to the reviewers for useful suggestions and corrections.

AUTHOR DECLARATIONS

Conflict of Interest

The authors have no conflicts to disclose.

[a]Electronic mail: mlittman@princeton.edu, ORCID: 0000-0002-8407-8053.
[b]Present address: Physics and Computer Science, Cornell University, Ithaca, NY 14850, ORCID: 0000-0002-9847-0232.
[c]Present address: Physics, Harvard University, Cambridge, MA 02138, ORCID: 0000-0003-1019-8375.
[d]Present address: Terra Global Capital, LLC, Oakland, CA 94611.

[1]N. Bohr, "On the constitution of atoms and molecules," Philos. Mag. **6**(26), 1–25 (1913).
[2]J. R. Rydberg, "On the structure of the line-spectra of the chemical elements," London, Edinburgh, Dublin Philos. Mag. J. Sci. **29**(179), 331–337 (1890).
[3]M. Planck, "Ueber das gesetz der energieverteilung im normalspectrum [On the law of distribution of energy in the normal spectrum]," Ann. Phys. **309**(3), 553–563 (1901).
[4]Bohr's 1913 paper (Ref. 1) uses the CGS form of Coulomb's law. Coulomb's constant, $1/(4\pi\varepsilon_0)$, does not appear. We have added this constant in the text even though it does not appear explicitly in Bohr's formulation. This assures that the formula listed in the text is correctly stated in SI and CGS systems.

[5]L. de Broglie, "Recherches sur la theorie des quanta," Ann. Phys. **3**(10), 22–128 (1925).
[6]R. G. Hulet and D. Kleppner, "Rydberg atoms in circular states," Phys. Rev. Lett. **51**, 1430–1433 (1983).
[7]R. Karam, "Why are complex numbers needed in quantum mechanics? Some answers for the introductory level," Am. J. Phys. **88**(39), 39–45 (2020).
[8]K. W. Ford, "Niels Bohr's first 1913 paper: Still relevant, still exciting, still puzzling," Phys. Teach. **56**, 500–502 (2018).
[9]E. Schrödinger, "An undulatory theory of mechanics of atoms and molecules," Phys. Rev. **28**(6), 1049–1070 (1926).
[10]A. Sommerfeld, "Zur quantentheorie der spektrallinien," Ann. Phys. **51**, 1–94 (1916).
[11]A. Sommerfeld, *Atombau und Spektrallinien* (Freidrich Vieweg und Sohn, Braunschweig, 1919); translation by H. L. Brose, *Atomic Structure and Spectral Lines* (Methuen, London, 1923).
[12]T. Deeney and C. O. O'Sullivan, "Sommerfeld's elliptical atomic orbitals revisited - A useful preliminary to the study of quantum mechanics," Am. J. Phys. **82**(9), 883–886 (2014).
[13]J. Arnold, "The convergence of semi-classical and quantum mechanics: Examining atomic radiation through the lens of the correspondence principle," Undergraduate thesis, Princeton University, 2020.
[14]H. A. Bethe and E. E. Salpeter, *Quantum Mechanics of One and Two Electron Atoms* (Springer, Berlin, 1957).
[15]M. W. Horbatsch, E. A. Hessels, and M. Horbatsch, "Classical calculation of the lifetimes and branching ratios for radiative decays of hydrogenic atoms," Phys. Rev. A **71**, 020501-R (2005).
[16]J. D. Jackson, *Classical Electrodynamics*, 3rd ed. (Wiley, New York, 1999), ISBN: 0-471-30932-X, problems 14.21 and 14.22.
[17]A. Martin-Ruiz, J. Bernal, A. Frank, and A. Carbajal-Dominguez, "The classical limit of the quantum Kepler problem," J. Mod. Phys. **4**(6), 818–822 (2013).
[18]D. Savransky, E. Cady, and N. J. Kasdin, "Parameter distributions of Keplerian orbits," Ast. Jour. **728**, 66–72 (2013).
[19]D. Kleppner, M. Littman, and M. Zimmerman, "Highly excited atoms," Sci. Am. **244**(5), 130–149 (1981).
[20]E. G. P. Rowe, "The classical limit of quantum mechanical hydrogen radial distributions," Eur. J. Phys. **8**, 81–87 (1987).

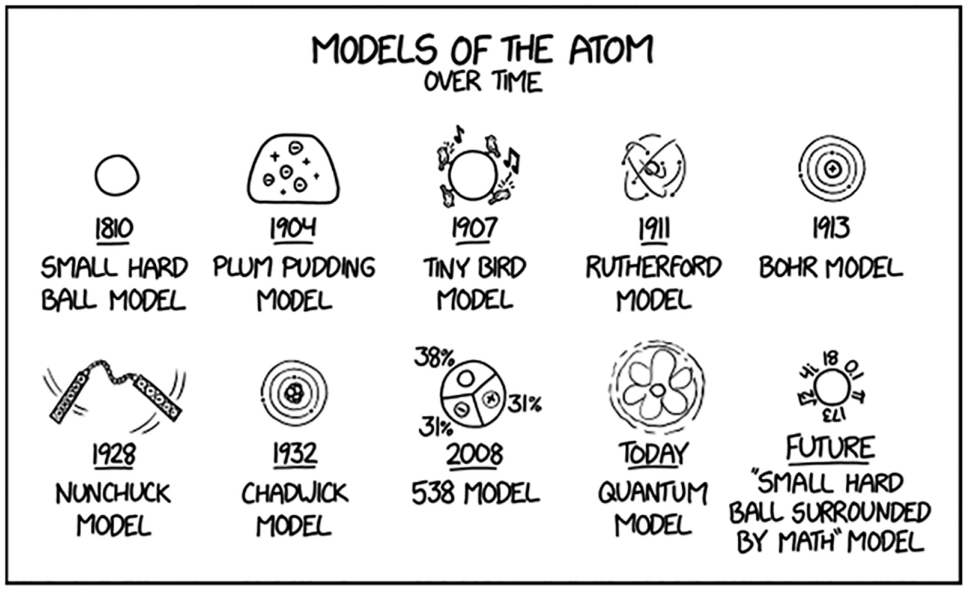

J.J. Thompson won a Nobel Prize for his work in electricity in gases, but was unfairly passed over for his "An atom is plum pudding, and plum pudding is MADE of atoms! Duuuuude." theory.
(Source: https://xkcd.com/2100)